Small-scale effect on the mechanical properties of metallic nanotubes

Jin Zhang, Chengyuan Wang,[a] Rajib Chowdhury, and Sondipon Adhikari
College of Engineering, Swansea University, Singleton Park, Swansea, Wales SA2 8PP, United Kingdom

(Received 24 June 2012; accepted 14 August 2012; published online 30 August 2012)

The residual stress and elastic modulus for the surface and core layers of metallic nanotubes (*MNT*s) are studied based on molecular dynamics simulations. The resultant small-scale effect is then demonstrated in a case study on the vibration of *MNT*s. In contrast to previous assumptions, it is found that the residual stresses at the inner and outer surfaces differ by several times and change sensitively with the geometric size of *MNT*s. In addition, the core layer stress ignored in most previous studies can also exert substantial influence on the structural response of *MNT*s. It is believed that these results can provide important guidance for the future study and potential applications of *MNT*s. © *2012 American Institute of Physics*. [http://dx.doi.org/10.1063/1.4748975]

Metallic nanotubes (*MNT*s) (Fig. 1) have attracted considerable attention owing to their great potential for constructing nanodevices and nanoelectronics, such as ultrasmall sensors, ultrahigh density recording media, and drug (gene) delivery.[1–4] They also offer an opportunity to advance the physics associated with their fabrication and applications. Recently, the smallest possible *MNT* with a square cross-section has been synthesized, which can be transformed into an exotic structure due to applied stress and dynamics.[5,6] The observation provides an impetus to reveal the formation mechanisms of the unexpected structure. A more fundamental issue on *MNT*s is their unique mechanical properties. These play a key role in their potential applications and thus have excited a significant wave of studies recently.[7–10]

For nanoscale structures like *MNT*s, the surface-to-volume ratio is greatly raised relative to that of their macroscopic counterparts, which would dramatically enhance the surface effect and finally lead to the size-dependent mechanical responses. To capture this small-scale effect, a core-surface (CS) model considering the effect of the surface properties has been proposed and widely used to predict the structural responses of solid nanowires (*NW*s),[11–14] nanofilms (*NF*s),[15–18] and hollow *MNT*s.[19,20] It thus becomes essential to accurately measure the surface properties of existing nanostructures. Initial attempts were made to obtain the surface stress and elastic modulus for some *NW*s and *NF*s based on atomistic simulations or experiments.[21–24] Nevertheless, their possible size-dependence has not been examined so far. In particular, the surface properties of *MNT*s are not yet available in the literature despite the fact that hollow nanostructures possess an even larger surface-to-volume ratio. Thus, when the CS model was used for *MNT*s,[19,20] it was tacitly assumed that the inner and outer surface layers of *MNT*s have the same properties as those of solid *NW*s. This could lead to large errors as the inner and outer surfaces have different average coordination numbers.[25] Furthermore, the surface residual stress would induce an initial stress in the inner section due to the deformation compatibility. This stress however was completely ignored in most previous studies although it could play a significant role in the structural responses at the nanoscale.[26] These fundamental issues on the small-scale effect are indeed of major concerns in nanomechanics and thus deserve a detailed study.

In this Letter, molecular dynamics simulations (MDS) were employed to study the mechanical properties of the surface layers and core layer of *MNT*s, e.g., residual stress, Young's modulus and their dependence on the size of *MNT*s. The obtained properties were then entered into a modified CS model to examine the small-scale effect on the elastic properties and the structural response of *MNT*s.

In the present study, copper *MNT*s of a square cross-section are considered with a $\langle 100 \rangle$ longitudinal orientation and $\{100\}$ transverse side surface (Fig. 1). The outer cross-sectional length l of the *MNT*s is fixed at $l = 5.5a$ ($a = 0.361$ nm is the lattice constant of bulk fcc copper), whereas the inner cross-sectional length l_0 varies between $1.5a$ and $3.5a$. To characterise the mechanical behaviour of the *MNT*s under the umbrella of continuum theory, a surface-core-surface model (Fig. 1) is employed where the mechanical properties for the outer and inner surface layers and the core layer will be calculated based on MDS. Here, the embedded atom potential proposed in Ref. 27 is used in the MDS to describe the atomic interactions in copper. In the present study, MDS are performed via following steps: The atoms were first brought to the positions corresponding to the lowest energy. Subsequently, a Nosé-Hoover thermostat[28] was applied to thermally equilibrate the atoms at 1 K to reduce thermal vibration effect. After the full relaxation, the *MNT*s would then be quasistatically loaded in tension in the axial direction. In this process, one end of the *MNT*s was fixed and the other end was pulled along the axial direction. This created a ramp velocity profile where the velocity rises from zero at the fixed end to its maximum value at the free end. Following Ref. 7, we choose a relatively low strain rate of $10^9\,s^{-1}$ to avoid the crystalline defects normally precluded due to a high rate of loading. The present MDS were conducted using large molecular dynamics simulator (LAMMPS)[29] with periodic boundary conditions along axial direction. The surface directions were kept free.

Using the above-mentioned method, we first calculated the distribution of the residual stress on the cross-sections of

[a]Author to whom correspondence should be addressed. Electronic mail: chengyuan.wang@swansea.ac.uk.

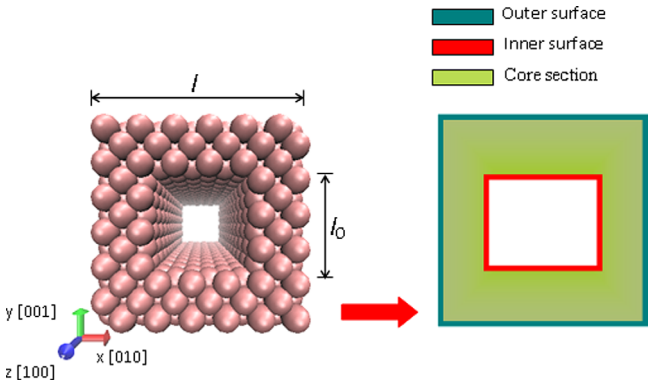

FIG. 1. Molecular representation of an *MNT* with a square cross-section and its equivalent core-surface model. The outer cross-section length is l and the inner cross-sectional length is l_0.

an (solid) *NW* and three *MNT*s (Fig. 2(a)) whose ratio l_0/l increases from 0 (the *NW*) to 0.27, 0.45, and 0.64. It is seen from Fig. 2(a) that nonuniform residual stress is found throughout the cross-sections of the *NW* and *MNT*s. The magnitude of the residual stress is of the order of gigapascal. Let us have a look at the *NW* (e.g., $l_0/l = 0$) for instance. The maximum residual tension about 8.5 GPa is found on the outer surface and the maximum residual compression around 2 GPa is obtained at the central part. The results are found to be in a good agreement with the results (−2 to 9 GPa) obtained by Wu for copper *NW* of the same geometric size.[30] Furthermore, it is noted in Fig. 2(a) that the magnitude of the stress at the innermost and outermost one-atom layers differs substantially from the stress in the core section, which is nonzero and almost uniformly distributed. This stress distribution shows clearly that, similar to what stated in Refs. 31 and 32, the outermost and the innermost one-atom layer can be considered as the outer and inner surfaces of *MNT*s. The effective thickness of the surface layers can then be defined as half of the lattice constant at the temperature considered.[32]

Next, we further calculated the average residual stress as a function of the ratio l_0/l for the inner, outer surface layers and the core layer individually. As pointed out in Ref. 33, the residual stress at the surface layer (s) remains a standard tensor quantity. However, since the thinnest possible surface layers in the plane-stress state are considered only the in-plane surface stresses (the membrane stresses) are nonzero whereas all off-plane stresses vanish. In particular, the normal in-plane surface stress is assumed to be identical in all directions and accordingly, the shear stresses at the thin surface layer (s) go to zero. The normal axial stresses obtained at the surface layers and the core layer are presented in Fig. 2(b) where the solid lines represent tensile stresses while the dashed lines denote compressive ones. It is noted in the figure that the residual stress on the outer surface τ_o is much larger than the stress on the inner surface τ_i. For example, at $l_0/l = 0.27$, τ_i is about 1 GPa, while τ_o reaches 7.1 GPa, which is seven times of τ_i. Moreover, in Fig. 2(b), τ_o is always a tensile stress and decreases monotonically as the ratio l_0/l increases, i.e., the rectangular hole becomes larger. On the other hand, τ_i is a tensile stress only at small l_0/l. Its magnitude then decreases as l_0/l grows and goes to zero when l_0/l reaches a critical value around 0.5. When l_0/l exceeds this critical value, i.e., the inner hole further expands, τ_i turns out to be a compressive stress whose magnitude increases as l_0/l rises. From these results, it follows that both τ_o and τ_i change sensitively with the variation of l_0/l but their dependences on l_0/l are qualitatively different. This finding is in sharp contrast to the assumption that τ_o and τ_i of *MNT*s are identical and independent of l_0/l.[19,20] In addition, a compressive stress σ_b is obtained in the core layer, which grows from 2.1 to 3.6 GPa with rising l_0/l and is generated primarily due to the deformation comparability in the *MNT*s (or *NW*). Here, the equilibrium of *MNT*s (*NW*) requires that the resultant force of τ_o, τ_i, and σ_b on the cross-section goes to zero.

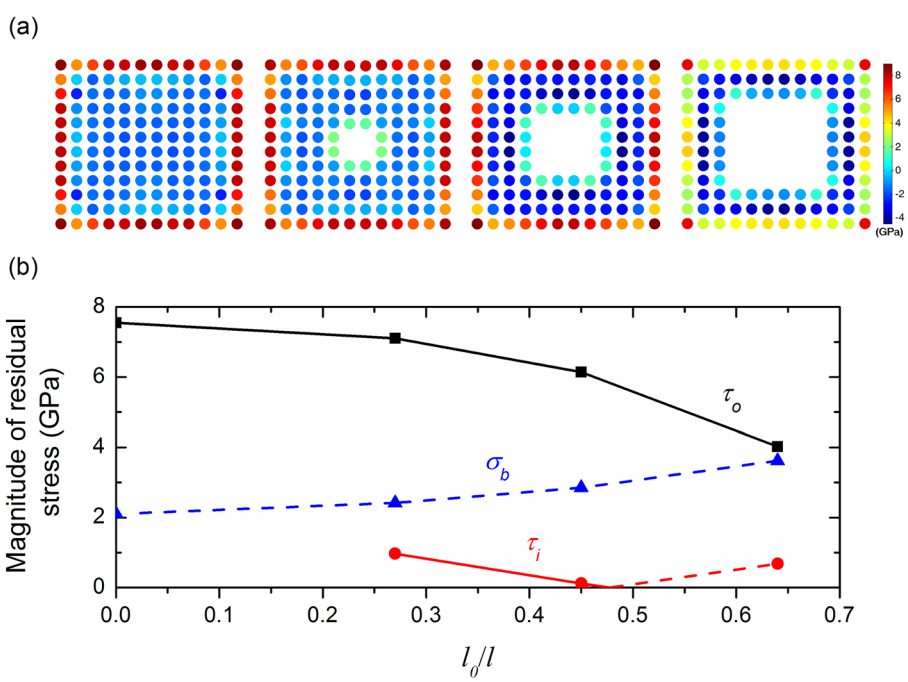

FIG. 2. (a) The cross-sectional stress distribution of an *NW* and *MNT*s; (b) Surface stresses of the *NW* and *MNT*s with different ratios l_0/l. Here, the solid lines represent the tensile stresses and the dashed lines represent the compressive stresses. The outer cross-sectional length l of the *NW* and *MNT*s is fixed at $5.5a$ where $a = 0.361$ nm.

In addition to the residual stresses, we are also interested in studying elastic moduli of individual layers and estimating their effect on the equivalent Young's modulus of *MNT*s. To this end, the linear stress-strain relation was calculated for *MNT*s in Fig. 3(a), where the small strain $\varepsilon \leq 1\%$ was considered. The slope of a straight line in Fig. 3(a) gives the equivalent Young's modulus of the corresponding *MNT*. It is found that the equivalent Young's modulus of whole *MNT*s decreases by 14% as the ratio l_0/l increases from 0 to 0.64. Similar calculation was done in Fig. 3(b) to quantify the Young's modulus of the inner, outer surface layers and the core layer, individually. It is noted in Fig. 3(b) that the Young's moduli of the inner and outer surface layers are quite close to each other but they are much lower than that of the core section. To get some ideas, at $l_0/l = 0.27$, Young's modulus of the core section is 70 GPa, which is about two times as much as that of the inner (35 GPa) and outer surface layer (37 GPa). Also, in Fig. 3(b), Young's modulus of the three sections increases with rising l_0/l. They rise less than 10% when l_0/l goes from 0 to 0.64.

Here, it is noted that the reversed l_0/l-dependence of Young's modulus is achieved for *MNT*s and their three constituent layers. To understand this observation, the Young's modulus of *MNT*s given by MDS in Fig. 3(a) are compared with those predicted based on (1) the CS model and (2) the Young's moduli obtained in Fig. 3(b) for the individual layers of *MNT*s. In the CS model, an *MNT* is modeled as a composite beam whose equivalent Young's modulus Y can be calculated by $Y = E_i v_i + E_o v_o + E_b v_b$.[32] Here, E and v are elastic moduli and volumetric fraction of individual layers. The subscripts i, o, and b, respectively, represent the parameter of the inner, outer surface layers and the core section. A good agreement is achieved in Fig. 3(c) between the MDS and the CS model, suggesting that the size-dependence of the equivalent Young's modulus Y is due to the effect of the surface elasticity. Specifically, the decrease of Y with rising l_0/l is primarily a result of the increasing volumetric fractions (v_i and v_o) of the surface layers, where E_i and E_o are much lower than E_b. Here, the tendency of Y obtained in Fig. 3(c) based on the present MDS is found to be in accordance with the simulations given in Ref. 8 for copper *MNT*s.

Finally, to demonstrate the importance of the above-obtained properties, we examined their effects on the transverse vibration of *MNT*s. The analysis was carried out based on the CS model where an *MNT* is considered as a composite Euler-Bernoulli beam. The beam consists of the two surface layers and the core layer of an *MNT*, which are perfectly bonded at their interfaces. Different form previous studies,[19,20] the residual stress σ_b in the core layer is considered in the present CS model. The dynamic equation of such a composite beam can be derived as[34] $(YI)_e \partial^4 w/\partial x^4 - H\partial^2 w/\partial x^2 + \rho A \partial^2 w/\partial t^2 = 0$, where w denotes the deflection of the beam at position x and time t; ρ is the mass density and A is the area of the cross-section; $(YI)_e$ is the effective bending stiffness; and H is the additional axial force due to residual surface stress. Taking a simply supported *MNT* with a length $L = 25l$ as an example, the fundamental frequency can be obtained as $\omega = \sqrt{[\pi^4 (YI)_e/L^4 + \pi^2 H/L^2]/(\rho A)}$. Here, the small-scale effect on ω is measured by $\Delta = (\omega - \omega_0)/\omega_0$, where ω_0 is the fundamental frequency obtained without considering surface layers and residual stresses, i.e., $H = 0$ and $Y = E_b$ for the whole beam. Three sets of results are plotted in Fig. 4 against l_0/l, i.e., Δ_1 obtained by using the surface properties (τ_o, τ_i, E_o, and E_i) and residual stress in the core layer σ_b, Δ_2 calculated by considering the above surface properties only but assuming $\sigma_b = 0$, and Δ_3 obtained based on the assumption[19,20] that $\sigma_b = 0$ and the properties of the two surfaces are identical and equal to those associated with $l_0/l = 0$. The curve representing Δ_1 is enlarged in the inset of Fig. 4. It is shown in the inset that when l_0/l increases from 0.27 to 0.45

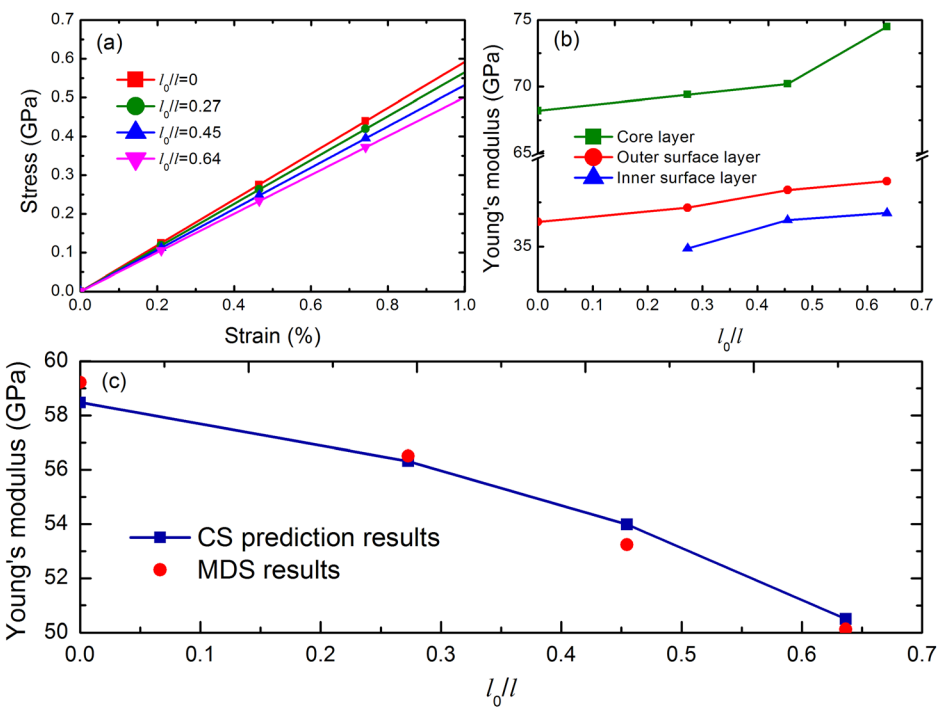

FIG. 3. (a) Stress-strain curves for *MNT*s with different ratios l_0/l; (b) Effective Young's modulus for the three regions of the *MNT*s as a function of the ratio l_0/l; (c) the equivalent Young's modulus of the *MNT*s as a function of the ratio l_0/l from the MDS and the CS model.

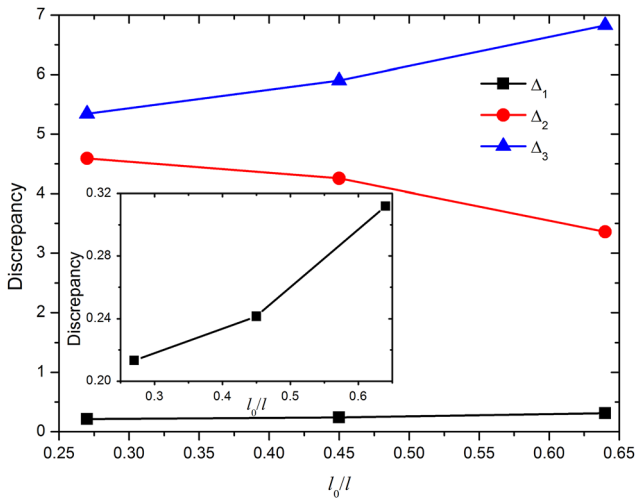

FIG. 4. The relative change of fundamental frequency $\Delta = (\omega - \omega_0)/\omega_0$ obtained for an *MNT* ($L = 25l$, $l = 5.5a$, and $a = 0.361$ nm) as a function of the ratio l_0/l. The result Δ_1 is given by the present CS model with considering stress at core layer, Δ_2 is obtained based on the present CS model without considering stress at core layer, and Δ_3 is obtained based on the previous CS model.

and to 0.64, Δ_1 grows from 21% to around 32% showing that the small-scale effect is significant and increase considerably with rising area of the inner surface. In the same process, Δ_2 falls in the ranges of (3.4, 4.3), which is an order of magnitude greater than Δ_1. This shows that the effect of σ_b is large and thus should be considered in predicting structural responses of the *MNT*s. Moreover, in Fig. 4, Δ_3 in the range of (5.3, 6.4) is even greater than Δ_2 indicating that the CS mode based on the assumption in Refs. 19 and 20 is oversimplified and would greatly overestimate the small-scale effect on *MNT*s.

In summary, molecular dynamics simulations were performed to study the residual stress and elastic modulus of the surface and core layers of copper *MNT*s. A tensile stress is obtained at the outer surface, which induces a compressive stress in the core layer. However, either tension or compression can be achieved at the inner surface and its magnitude is several times smaller than that at the outer surface. The size-dependence of the residual stresses is significant but qualitatively different for the three layers of *MNT*s. In addition, Young's moduli of the two surfaces are close and much lower than that of the core layer. This leads to the equivalent Young's modulus of *MNT*s decreasing with the rising area of the surfaces. It is shown in a case study that the small-scale effect originating from the residual stresses and surface elasticity is crucial for accurately characterizing the structural responses of *MNT*s.

J.Z. acknowledges the support from the China Scholarship Council (CSC). S.A. acknowledges the support from the Royal Society through the award of Wolfson Research Merit Award.

[1]J. J. Krebs, M. Rubinstein, P. Lubitz, M. Z. Harford, S. Baral, R. Shashidhar, Y. S. Ho, G. M. Chow, and S. Qardri, J. Appl. Phys. **70**, 6404 (1991).
[2]S. Khizroev, M. H. Kryder, D. Litvinov, and D. A. Thompson, Appl. Phys. Lett. **81**, 2256 (2002).
[3]A. K. Salem, P. C. Searson, and K. W. Leong, Nature Mater. **2**, 668 (2003).
[4]S. F. Yu, S. B. Lee, and C. R. Martin, Anal. Chem. **75**, 1239 (2003).
[5]M. J. Lagos, F. Sato, J. Bettini, V. Rodrigues, D. S. Galvao, and D. Ugarte, Nat. Nanotechnol. **4**, 149 (2009).
[6]P. A. S. Autreto, M. J. Lagos, F. Sato, J. Bettini, A. R. Rocha, V. Rodrigues, D. Ugarte, and D. S. Galvao, Phys. Rev. Lett. **106**, 065501 (2011).
[7]C. J. Ji and H. S. Park, Appl. Phys. Lett. **89**, 181916 (2006).
[8]C. J. Ji and H. S. Park, Nanotechnology **18**, 115707 (2007).
[9]Y. G. Zheng, H. W. Zhang, Z. Chen, L. Wang, Z. Q. Zhang, and J. B. Wang, Appl. Phys. Lett. **92**, 041913 (2008).
[10]S. Jiang, H. W. Zhang, Y. G. Zheng, and Z. Chen, J. Phys. D: Appl. Phys. **42**, 135408 (2009).
[11]G. F. Wang and X. Q. Feng, Appl. Phys. Lett. **90**, 231904 (2007).
[12]J. He and C. M. Lilley, Nano Lett. **8**, 1798 (2008).
[13]J. He and C. M. Lilley, Appl. Phys. Lett. **93**, 263108 (2008).
[14]G. F. Wang and X. Q. Feng, Appl. Phys. Lett. **94**, 141913 (2009).
[15]A. Assadi, B. Farshi, and A. Alinia-Ziazi, J. Appl. Phys. **107**, 124310 (2010).
[16]J. Choi, M. Cho, and W. Kim, Appl. Phys. Lett. **97**, 171901 (2010).
[17]J. Zhang and C. Y. Wang, J. Appl. Phys. **111**, 094303 (2012).
[18]J. Zhang, C. Y. Wang, and S. Adhikari, J. Phys. D: Appl. Phys. **45**, 285301 (2012).
[19]B. Farshi, A. Assadi, and A. Alinia-Ziazi, Appl. Phys. Lett. **96**, 093105 (2010).
[20]H. L. Lee and W. J. Chang, J. Appl. Phys. **108**, 093503 (2010).
[21]R. E. Miller and V. B. Shenoy, Nanotechnology **11**, 139 (2000).
[22]V. B. Shenoy, Phys. Rev. B **71**, 094104 (2005).
[23]G. Y. Jing, H. L. Duan, X. M. Sun, Z. S. Zhang, J. Xu, Y. D. Li, J. X. Wang, and D. P. Yu, Phys. Rev. B **73**, 235409 (2006).
[24]A. Asthana, K. Momeni, A. Prasad, Y. K. Yap, and R. S. Yassar, Nanotechnology **22**, 265712 (2011).
[25]C. Q. Sun, B. K. Tay, X. T. Zeng, S. Li, T. P. Chen, J. Zhou, H. L. Bai, and E. Y. Jiang, J. Phys.: Condens. Matter **14**, 7781 (2002).
[26]F. Song, G. L. Huang, H. S. Park, and X. N. Liu, Int. J. Solid Struct. **48**, 2154 (2011).
[27]M. Doyama and Y. Kogure, Comput. Mater. Sci. **14**, 80 (1999).
[28]S. Nosé, J. Chem. Phys. **81**, 511 (1984).
[29]S. J. Plimpton, J. Comput. Phys. **117**, 1 (1995).
[30]H. A. Wu, Mech. Res. Commun. **33**, 9 (2006).
[31]G. Ouyang, C. X. Wang, and G. W. Yang, Chem. Rev. **109**, 4221 (2009).
[32]B. M. Gong, Q. Chen, and D. P. Wang, Mater. Lett. **67**, 165 (2012).
[33]M. E. Gurtin and A. I. Murdoch, Arch. Ration. Mech. Anal. **57**, 291 (1975).
[34]See supplementary material at http://dx.doi.org/10.1063/1.4748975 for the derivation of the dynamic equations and the fundamental frequency used in the Letter.